Order−Order and Order−Disorder Transitions in a Polystyrene-*block*-Polyisoprene-*block*-Polystyrene Copolymer

Naoki Sakamoto and Takeji Hashimoto*

Department of Polymer Chemistry, Graduate School of Engineering, Kyoto University, Kyoto 606-01, Japan

Chang Dae Han,* Do Kim, and Nitin Y. Vaidya

Department of Polymer Engineering, The University of Akron, Akron, Ohio 44325-0301

Received April 24, 1996; Revised Manuscript Received January 23, 1997[⊗]

ABSTRACT: We investigated the order−order transition (OOT) and the order−disorder transition (ODT) in a polystyrene-*block*-polyisoprene-*block*-polystyrene copolymer (Vector 4111, Dexco Polymers Co.), which has a weight-average molecular weight of 1.4×10^5 and a 0.183 weight fraction of polystyrene (PS) blocks, using small-angle X-ray scattering (SAXS) and rheological measurements. Specifically, SAXS experiments reveal that Vector 4111 undergoes an OOT at 179−185 °C with (i) hexagonally-packed cylindrical microdomains of PS at $T \leq 179$ °C, (ii) the coexistence of cylindrical and spherical microdomains of PS at 180 °C $\leq T \leq$ 185 °C, and (iii) spherical microdomains of PS in a cubic lattice at 185 °C $< T \leq$ 210 °C, and (iv) the cubic lattice of the spheres is distorted with a further increase of temperature so that the lattice disordering transition occurs at temperatures between 210 (onset) and 214 °C (completion) and the spherical microdomain structure of PS with a liquidlike short-range order persists even up to 220 °C, the highest experimental temperature employed. The SAXS results are confirmed by independent rheological measurements. Transmission electron microscopy (TEM) was employed to investigate the microdomain structures of Vector 4111 at elevated temperatures by rapidly quenching specimens, which had been annealed at a predetermined temperature, into ice water. TEM results reveal that (i) at 170 °C Vector 4111 has hexagonally-packed cylindrical microdomains of PS, (ii) at 185 °C the cylindrical and spherical microdomains of PS coexist, and (iii) as the temperature is increased further to 220 °C, only spherical microdomains of PS persist; i.e., the order−disorder transition temperature (T_{ODT}) of Vector 4111 is higher than 220 °C. We found from the present study that the dynamic temperature sweep experiment under isochronal conditions failed to accurately determine the T_{ODT} of Vector 4111 having a low volume fraction of PS blocks, while log G' vs log G'' plots were very effective to investigate both OOT and ODT in Vector 4111.

1. Introduction

During the past 2 decades, scattering and rheological methods have been used extensively to investigate the order−disorder transition (ODT) in block copolymers. There are too many papers to cite all of them here, and interested readers are referred to two review papers[1,2] and a recent paper by Han et al.[3]

Only within the past 3 years have the experimental observations of order−order transitions (OOTs) in block copolymers been reported,[4−10] although it was first predicted 15 years ago by Leibler.[11] Specifically, using small-angle X-ray scattering (SAXS) and transmission electron microscopy (TEM), Sakurai et al.[4] observed a thermally induced OOT from cylindrical to lamellar microdomains in a polystyrene-*block*-polybutadiene-*block*-polystyrene (SBS triblock) copolymer. Using SAXS, Sakurai et al.[5] observed that a polystyrene-*block*-polyisoprene (SI diblock) copolymer had hexagonally-packed cylindrical microdomains at 150 °C and spherical microdomains in a body-centered cubic lattice (bcc) at 200 °C. Using specimens which had different thermal histories at elevated temperatures (150 and 200 °C, respectively) followed by rapid quenching in ice water, they confirmed via TEM the reversible nature of OOT from cylindrical to spherical microdomains and from spherical to cylindrical microdomains in the SI diblock copolymer. Using SAXS and TEM, Hajduk et al.[6] also observed a thermally reversible morphological transition between cylinders and lamellae in a polystyrene-*block*-poly(ethylene butene) copolymer. In a series of papers, Bates and co-workers[7−10] reported on OOTs in poly(ethylenepropylene)-*block*-poly(ethylethylene) (PEP−PEE diblock) and SI diblock copolymers, using rheology, SAXS, small-angle neutron scattering (SANS), and/or TEM.

In the use of rheological measurements to investigate ODTs or OOTs in block copolymers, two types of rheological experiments are usually conducted: (a) a dynamic temperature sweep experiment under isochronal conditions and (b) a dynamic frequency sweep experiment at various temperatures.

There are too many references, which describe rheological experiments to determine the order−disorder transition temperature (T_{ODT}) of block copolymers, to cite them all here, and interested readers are referred to a very recent paper by Han et al.[3] and references therein. As will be shown in this paper, the two types of rheological measurements do not always give rise to the same value of T_{ODT}, especially for highly asymmetric block copolymers.

When using the dynamic temperature sweep experiment under isochronal conditions, Bates and co-workers[7−10] determined the order−order transition temperature (T_{OOT}) of a block copolymer by identifying the temperature at which G' goes through a minimum. Interestingly enough, for certain PEE−PEP diblock copolymers investigated by Almdal et al.[7] and SI diblock copolymers investigated by Khandpur et al.,[10] various ordered phases were observed as manifested by multiple minima in G' with respect to temperature, and the observations were confirmed by TEM, SAXS, and/or

[⊗] Abstract published in *Advance ACS Abstracts,* March 1, 1997.

S0024-9297(96)00610-9 CCC: $14.00 © 1997 American Chemical Society

SANS. While investigating the OOT in SI diblock copolymer, Khandpur et al.[10] observed, besides the well-known spheres, hexagonally-packed cylinders, and lamellae, two additional microdomain structures, hexagonally-perforated layers and a bicontinuous cubic phase.

Very recently, we investigated the OOT and ODT in a polystyrene-*block*-polyisoprene-*block*-polystyrene (SIS triblock) copolymer (Vector 4111) by SAXS and rheological measurements. SAXS measurements revealed that Vector 4111 undergoes an OOT from hexagonally-packed cylindrical to spherical microdomains of polystyrene (PS) in a cubic lattice (either bcc or face-centered cubic (fcc) with considerable lattice distortion) at temperatures between 179 (onset of OOT) and 185 °C (completion of OOT). Upon a further increase in temperature, the system exhibits a lattice-disordering transition (LDT) at temperatures between 210 (onset of LDT) and 214 °C (completion of LDT) and it has a T_{ODT} higher than 220 °C, which is supported by TEM and rheological measurements, respectively. In this paper, we define the T_{ODT} as a temperature above which the spherical microdomains disappear. We are aware of the fact that within the spirit of the mean-field theory of Leibler,[11] LDT coincides with ODT. However, as will be elaborated on in this paper, we distinguish LDT from ODT for the Vector 4111 investigated in this study, because we observed, via SAXS, spherical microdomains at temperatures above the lattice-disordering transition temperature (T_{LDT}) and below the T_{ODT} of Vector 4111. We define the T_{ODT} of Vector 4111 to be the temperature at which spherical microdomains disappear and a single-phase state is attained in the system. In this paper, we present the highlights of our findings.

2. Experimental Section

2.1. Material. In this study, a commercial grade (Vector 4111, Dexco Polymers Co.) of SIS triblock copolymer was employed. We determined (i) the weight-average molecular weight to be 1.4×10^5 via light scattering, (ii) the weight fraction of PS blocks to be 0.183 via nuclear magnetic resonance spectroscopy, and (iii) the polydispersity index (M_w/M_n) to be 1.11 via gel permeation chromatography.

2.2. Sample Preparation. Samples were prepared by first dissolving a predetermined amount of Vector 4111 (10 wt %) in toluene in the presence of an antioxidant (Irganox 1010, Ciba-Geigy Group) and then slowly evaporating the solvent. The evaporation of solvent was carried out slowly at room temperature for 1 week and then in a vacuum oven at 40 °C for 3 days. The last trace of solvent was removed by drying the samples in a vacuum oven at an elevated temperature by gradually raising the oven temperature from 40 to 110 °C at a rate of 10 °C/h. The drying of the samples was continued, until there was no further change in weight, and then the specimens were stored in a refrigerator.

2.3. SAXS Experiments. SAXS experiments were conducted under a nitrogen atmosphere in the heating and cooling cycles, using an apparatus described in detail elsewhere,[12] which consists of a newly replaced 18-kW rotating-anode X-ray generator operated at 45 kV × 400 mA (MAC Science), a graphite crystal for incident-beam monochromatization, a 1.5-m camera, and a one-dimensional position-sensitive proportional counter. The Cu Kα line ($\lambda = 0.154$ nm) was used. The SAXS profiles were measured as a function of temperature and were corrected for absorption, air scattering, and background scattering arising from thermal diffuse scattering and slit-height and slit-width smearing.[13] The absolute SAXS intensity was obtained using the nickel-foil method.[14] In the present study, the temperature dependence of the SAXS profiles was obtained with a large temperature increment (referred to hereafter as the *low-temperature-resolution* SAXS experiment) and also with a small temperature increment (referred to hereafter as the *high-temperature-resolution* SAXS experiment) in a temperature enclosure which was sealed by nitrogen gas. This new temperature enclosure and temperature controller enabled us to control the sample temperature to within ±0.002 °C.

Table 1. Thermal Histories of the Specimens Used for TEM Experiment

sample code	thermal history
A	first annealed at 140 °C for 48 h and then heated to 170 °C and held there for 2 h followed by a rapid quenching in ice water
B	first annealed at 140 °C for 48 h and then heated to 185 °C and held there for 2 h followed by a rapid quenching in ice water
C	first annealed at 140 °C for 48 h and then heated to 200 °C and held there for 30 min followed by a rapid quenching in ice water
D	first annealed at 140 °C for 48 h and then heated to 220 °C and held there for 30 min followed by a rapid quenching in ice water

2.4. Rheological Measurement. In this study, a Rheometrics mechanical spectrometer (Model RMS 800) was used in the oscillatory mode with parallel-plate fixtures (25-mm diameter). Two different types of experiment were conducted. (1) Dynamic temperature sweep experiments were conducted; i.e., the dynamic storage modulus (G') was measured under isochronal conditions (at $\omega = 0.01$ and 0.1 rad/s) with temperature increasing (i.e., during heating) from 160 to 220 °C or decreasing (i.e., during cooling) from 220 to 160 °C at a rate of 0.4 °C/min. (2) Dynamic frequency sweep experiments were conducted, i.e., dynamic storage and loss moduli (G' and G'') were measured as functions of angular frequency (ω) ranging from 0.01 to 100 rad/s at various temperatures increasing from 160 to 220 °C during heating and decreasing from 220 to 160 °C during cooling. The temperature increment or decrement in the frequency sweep experiment varied from 3 to 10 °C, and the specimen was kept at a constant temperature for 30−40 min before rheological measurements actually began. The temperature control was accurate to within ±1 °C, and a fixed strain was used at a given temperature, to ensure that measurements were taken well within the linear viscoelastic range of the materials investigated. All the rheological measurements were conducted under a nitrogen atmosphere in order to avoid oxidative degradation of the samples.

In the present study, rheological measurements were *not* taken at temperatures above 220 °C, because an earlier study[15] indicated that appreciable cross-linking reactions may take place in SI diblock or SIS triblock copolymers at temperatures higher than 220 °C even in the presence of an antioxidant. Just before the temperature sweep or frequency sweep experiments for the heating or cooling cycles, an as-cast specimen was annealed either at 200 °C for 1 h or at 140 °C for 2 days. This was done in order to investigate whether or not different annealing conditions might affect the rheological responses.

2.5. TEM. TEM was conducted in order to determine the microdomain structure of Vector 4111 at elevated temperatures followed by rapid quenching in ice water. By having recognized the fact that the accuracy of the temperature at which specimens were annealed before rapid quenching was very crucial, a solvent-cast specimen was annealed in a specially designed vacuum oven (Yamato Scientific Co., Model DP-22) which can control the temperature to within ±1.5 °C up to 240 °C and can provide temperature uniformity inside the vacuum oven to within ±1.5 °C up to 240 °C. The temperature employed for annealing was guided by the rheological and SAXS studies. The thermal histories of the specimens used for TEM study are summarized in Table 1.

The ultrathin sectioning of the quenched specimens was performed by cryoultramicrotomy at −100 °C, below the glass transition temperature ($T_g = -68$ °C) of polyisoprene (PI), to attain the rigidity of the specimen, using a Reichert Ultracut S low-temperature sectioning system. A transmission electron microscope (JEM 1200EX II, JEOL) operated at 120 kV was used for taking the pictures of the specimens stained with osmium tetroxide vapor.

3. Results and Discussion

3.1. TEM Study. Figure 1 gives the micrographs of the Vector 4111 specimens, which were annealed at 170, 185, 200, and 220 °C, respectively, and then rapidly quenched into ice water in accordance with the thermal histories described in Table 1. We observe in Figure 1 that Vector 4111 has (i) hexagonally-packed cylinders at 170 °C, (ii) well-ordered cubic spheres at 185 and 200 °C, and (iii) distorted cubic spheres at 220 °C, respectively, indicating that the T_{ODT} of Vector 4111 is higher than 220 °C. As will be shown below, these observations are supported completely by the SAXS results and the rheological results, which indicate that Vector 4111 undergoes an OOT at a temperature in the vicinity of 182−185 °C and has a T_{ODT} above 220 °C. It should be noted, however, that we cannot rule out the possibility of ordering into spherical domains during quenching of the melt at 220 °C into ice water in a rigorous sense, unless the SAXS profiles before and after quenching are confirmed to be identical. This is left for future studies.

3.2. SAXS Study. Figure 2 summarizes schematically the temperature protocols employed (1) in the high-temperature-resolution SAXS experiments in the heating cycle from 170 to 185 °C (designated by thermal history l), (2) in the low-temperature-resolution SAXS experiments from 170 to 205 °C combined with the high-temperature-resolution experiments from 205 to 220 °C (designated by thermal history 2), and (3) in the high-temperature-resolution SAXS experiments in the cooling cycle from 220 to 204 °C combined with the low-temperature-resolution experiments from 200 to 165 °C (designated by thermal history 3). The *thick* horizontal solid lines represent the time during which the SAXS profiles were measured. For the SAXS study in the heating cycle reported here, as-cast Vector 4111 specimens were annealed at 200 °C for 1 h, but for the study in the cooling cycle, the as-cast specimens were used without annealing. As can be seen in Figure 2, in the low-temperature-resolution SAXS experiment during the heating cycle, an as-cast Vector 4111 specimen, which was placed in the temperature enclosure equilibrated at 200 °C, was cooled down slowly to 170 °C and then the specimen temperature was increased stepwise to 220 °C, while in the high-temperature-resolution SAXS experiment during the heating cycle, an as-cast Vector 4111 specimen, which was placed in the temperature enclosure equilibrated at 200 °C, was cooled slowly to 170 °C and then the specimen temperature was increased stepwise only to 185 °C. On the other hand, in the high-temperature-resolution SAXS experiment during the cooling cycle, the temperature of an as-cast Vector 4111 specimen was decreased stepwise from 220 to 165 °C.

The desmeared SAXS profiles obtained in the heating cycle are given in Figure 3. The details about the desmearing performed are given in a previous paper.[13] In Figure 3, we observe (a) a sharp OOT (see the upper panel) and (b) a sharp LDT taking place in the high-temperature-resolution SAXS experiment (see the lower panel). These transitions are sharp in the sense that they occur over a narrow temperature interval. It should be mentioned that each SAXS profile in panels a and b was shifted down along the vertical direction by 1 decade relative to the top profile in the respective panels. The following observations are worth noting in Figure 3: (1) at $T \leq 179$ °C, the specimen has the hexagonally-packed cylinders (see also Figure 1a) having the scattering maxima at $1:\sqrt{3}:\sqrt{4}$ relative to the position of the first-order maximum; (2) an onset of OOT takes place at $T > 179$ °C and OOT completes at $T < 185$ °C; (3) at 179 ° C $< T <$ 185 °C, the specimen has mixtures of hexagonally-packed cylindrical microdomains and spherical microdomains in the cubic lattice; i.e., the SAXS profiles consist of a composite of those from the two coexisting phases; (4) at 185 ° C $\leq T \leq$ 210 °C, the specimen has spherical microdomains in the cubic lattice (see also Figure 1b and 1c) having the scattering maximum at $1:\sqrt{2}:\sqrt{3}$ relative to the position of the first-order maximum, and the lattice is either bcc or fcc with a considerable lattice distortion; (5) an onset of LDT takes place at $T > 210$ °C and LDT completes at $T < 214$ °C; (6) at 214 °C $\leq T$, the specimen has spherical microdomains with "liquidlike" spatial order (i.e., liquidlike spheres) as detailed below; and (7) the thick arrow on the profile at 212 °C corresponds to the broad peak from the two peaks corresponding to $\sqrt{2}$ and $\sqrt{3}$ which overlap each other.

At this juncture, we would like to make a distinction between the LDT and the ODT for the Vector 4111 investigated in this study. Although one may be tempted to regard, in accordance with the mean-field theory of Leibler,[11] LDT as being equal to ODT and thus regard the system at temperatures above LDT as being in the disordered state, we do not believe that such a notion is acceptable to Vector 4111, because the existence of the spherical microdomains (see also Figure 1d), though arranged in a liquidlike short-range order, itself reveals that the state of the system is very different from the disordered state with thermal concentration fluctuations. We interpret the ordered phase with spherical microdomains having short-range order as being a consequence of the random thermal force, which perturbs the long-range order of a cubic lattice of the spheres. Although Leibler's mean-field theory predicts bcc structure just next to the disordered phase, we think that the random thermal force generates a new ordered phase with the spheres in a liquidlike short-range order in between the bcc phase and the disordered phase. Thus, in this paper, we will define the T_{ODT} of Vector 4111 as a temperature above which the spherical microdomains disappear and turn into thermal concentration fluctuations with a temperature-dependent characteristic relaxation time. We are of the opinion that the distinction between LDT and ODT made above is applicable *only* to block copolymers having spherical microdomains but *not* to block copolymers having cylindrical or lamellar microdomains.

The desmeared SAXS profiles obtained in the cooling cycle, the thermal history of which is designated as (3) in Figure 2, are given in Figure 4. The following observations are worth noting in Figure 4: (1) the specimen has liquidlike spherical microdomains as the temperature is decreased from 220 to 190 °C; (2) the broad maximum marked by an arrow indicates the broad maximum from the overlapped peaks of $\sqrt{2}$ and $\sqrt{3}$ from the distorted cubic lattice; (3) the SAXS profiles obtained at $T \leq 180$ °C show the scattering maximum at $1:\sqrt{3}:\sqrt{4}$ relative to the position of the first-order maximum, indicative of the presence of hexagonally-packed cylindrical microdomains; and (4) a sharp narrowing in the line profiles of the scattering maxima is discerned between 175 and 170 °C.

All the SAXS profiles in Figures 3 and 4 have a common asymptotic behavior of $I(q) \sim q^{-n}$, with n close to 4 at 0.27 nm$^{-1} \leq q \leq$ 0.6 nm^{-1}, as indicated by the first straight line of slope −4 drawn to each profile, together with the second straight line of slope −2. This indicates that the SAXS profiles at $T \geq 212$ °C in Figure

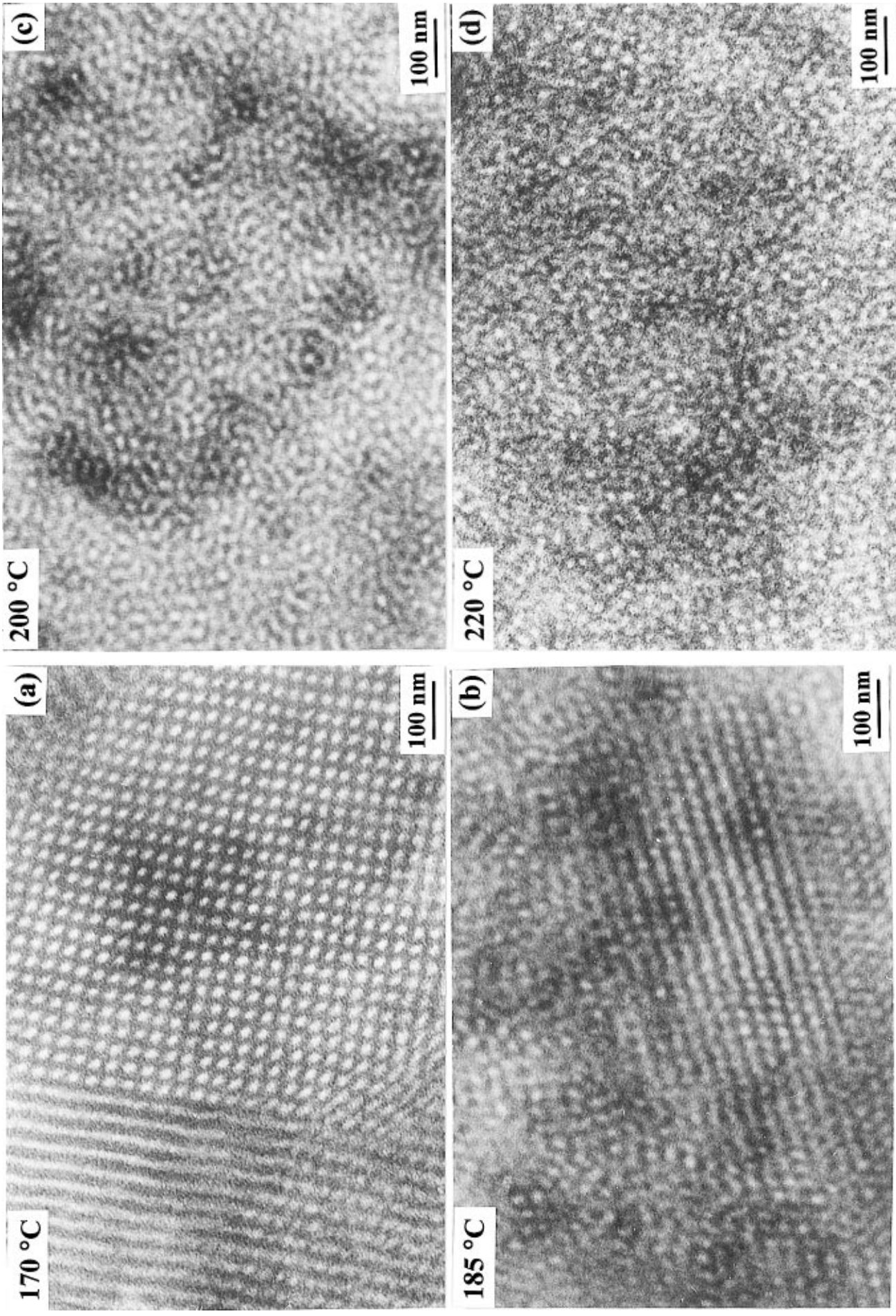

Figure 1. Transmission electron micrographs of Vector 4111 at 170, 185, 200, and 220 °C. These micrographs were taken after rapidly quenching the specimen from the respective temperatures into ice water, and the thermal histories of the specimens are summarized in Table 1.

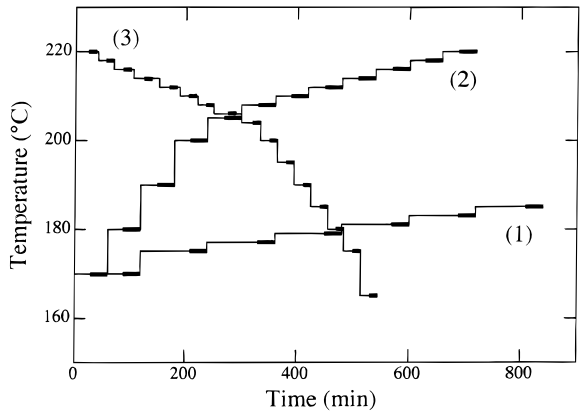

Figure 2. Schematic diagram describing the thermal histories of Vector 4111 specimens employed for SAXS experiments: curves 1 and 2 describe the temperature protocols during heating, and curve 3 describes the temperature protocol during cooling.

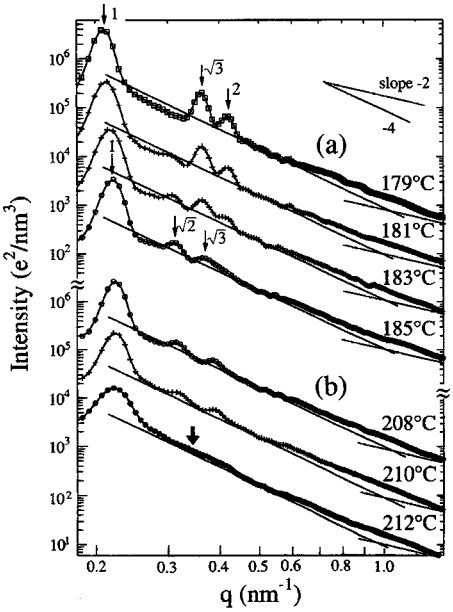

Figure 3. Temperature dependence of SAXS profiles for Vector 4111 during heating: (a) with temperature protocol 1 in Figure 2 and (b) with temperature protocol 2 in Figure 2, at various temperatures indicated on the plot. The straight line of slope −4 is drawn to each SAXS profile to show the asymptotic behavior of $I(q) \sim q^{-4}$, while the straight line of slope −2 is drawn to each SAXS profile as a guide to the eye for the crossover behavior from q^{-4} to q^{-2}.

3 and those at 190 °C < T < 220 °C in Figure 4, which have only the first-order peak as a well-defined peak, have the same asymptotic behavior as those with well-defined higher order peaks due to the hexagonally-packed cylinders or the spheres in the cubic lattice. This means that the SAXS profiles at the high temperatures arise from the microdomains with the same interface thickness as those with the hexagonally-packed cylinders and the spheres in the cubic lattice at lower temperatures. This strongly suggests the existence of spherical microdomains in the high-temperature range. However, the spatial distribution of centers of the spheres has only liquidlike short-range order as evidenced by the lack of well-defined higher order peaks at $\sqrt{2}$ and $\sqrt{3}$ relative to the first-order peak. The higher order peaks are overlapped into a very broad shoulder as marked by the thick arrows in Figures 3 and 4. The existence of the broad shoulder also suggests that the scattering in the high-temperature range is not

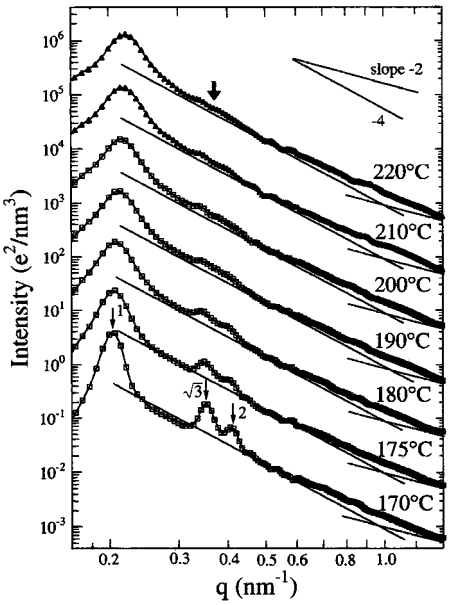

Figure 4. Temperature dependence of SAXS profiles for Vector 4111 during cooling with protocol 3 in Figure 2 at various temperatures indicated on the plot. The two straight lines drawn to each SAXS profile have the same physical meanings as those in Figure 3.

due to the thermal concentration fluctuations but rather due to the existence of spheres having short-range liquidlike spatial order. The existence of the spherical microdomains with a sharp interface was also supported by the evidence that the SAXS profiles at 0.27 $nm^{-1} \leq q \leq 0.6$ nm^{-1} in the high-temperature range can be fitted well with the theoretical profile from isolated spheres with a large size distribution, e.g., the SAXS profile at $T \geq 212$ °C with the spheres having a mean radius $R = 10.5$ nm and the standard deviation of 1.7 nm, although the calculated SAXS profile best fitted to the experimental profile is not included in this figure. The existence of the spherical microdomains in Vector 4111 at 220 °C is also evidenced by TEM (see Figure 1).

In reference to Figures 3 and 4, the upward deviation of each SAXS profile observed from the first straight line with the slope of −4 at $q \geq 0.6$ is expected to reflect a crossover from the Porod's law behavior of q^{-4} to the q^{-2} law due to the thermal concentration fluctuations within each domain. As q increases, the contribution of the scattering arising from the thermal fluctuations ($I(q) \sim q^{-2}$) dominates over that of the scattering arising from the interfaces ($I(q) \sim q^{-4}$), and hence, the SAXS profiles should eventually show the q^{-2} behavior at a sufficiently high q region. Unfortunately, however, our data do not quite reach the high-q region but rather terminate in the crossover q region. The second straight line of slope −2 is drawn as a guide to the eye for the crossover behavior.

Figure 5 gives plots of (a) the reciprocal of the first-order peak intensity ($1/I_m$) vs the reciprocal of the absolute temperature ($1/T$) and (b) the square of the half-width at half-maximum (σ_q^2) of the SAXS profile vs $1/T$ at temperatures ranging from 165 to 220 °C during the heating and cooling cycles, respectively. In Figure 5, (i) the symbol ● represents the data points taken during heating with temperature protocol 2 given in Figure 2, (ii) the symbol + represents the data taken during heating with temperature protocol 1 given in Figure 2, and (iii) the symbol ○ represents the data points taken during cooling with temperature protocol 3 given in Figure 2. From the SAXS data taken during

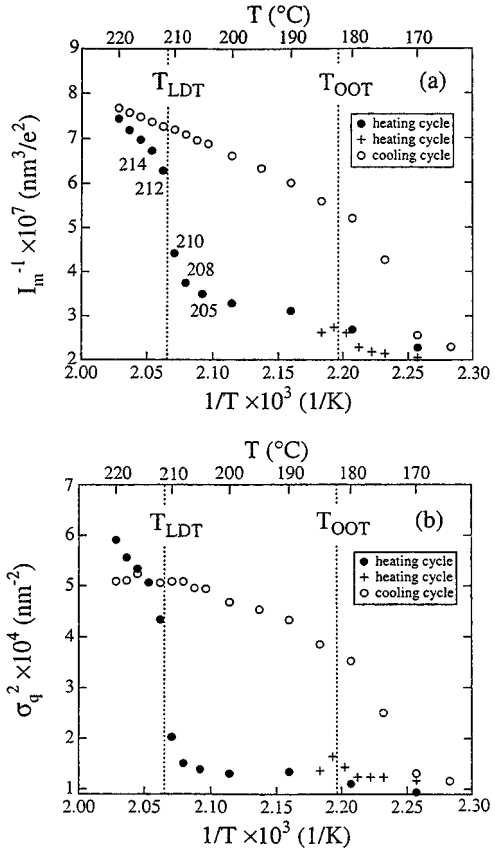

Figure 5. Plots of (a) $1/I_m$ vs $1/T$ and (b) σ_q^2 vs $1/T$ for Vector 4111: (●) low-temperature-resolution SAXS experiment during heating; (+) high-temperature-resolution SAXS experiment during heating; (○) high-temperature-resolution SAXS experiments during cooling. Three digit numbers attached to the data points (●) indicate temperatures in °C.

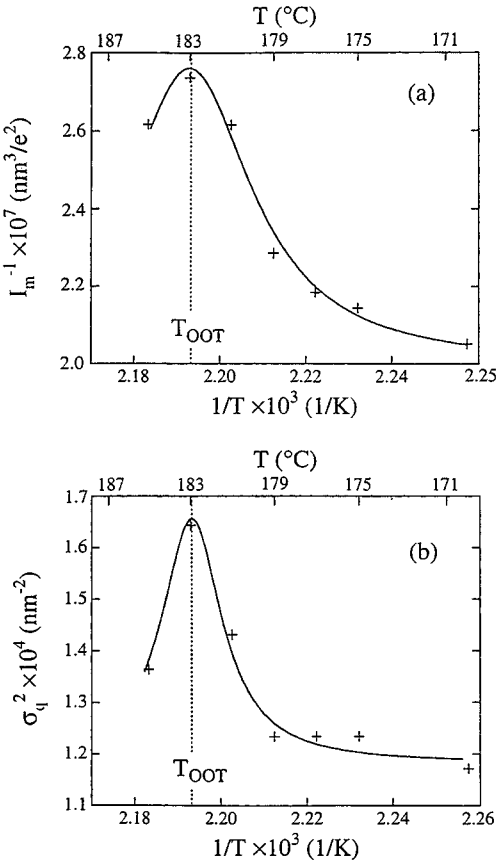

Figure 6. Plots of (a) $1/I_m$ vs $1/T$ and (b) σ_q^2 vs $1/T$ for Vector 4111 from high-temperature-resolution SAXS experiments during heating. The solid lines are for visual guides.

the heating cycle, represented by symbol ● in Figure 5, we observe a sharp discontinuous change in both $1/I_m$ vs $1/T$ and σ_q^2 vs $1/T$ plots at 212 °C. This change together with the change in the profile with T shown in Figure 3 illustrates that LDT occurs at around 212 °C. More precisely, the LDT occurs at temperatures between 210 (onset) and 214 °C (completion). This transition occurs in the narrow temperature interval (less than 4 °C) where the ordered sphere with a cubic lattice coexists with the liquid phase of the spheres. The LDT also causes the discontinuous change in D, as will be discussed below. On the other hand, in the time scale of our observation, we cannot discern the lattice formation transition (the reverse process of LDT) from the SAXS experiment performed during the cooling cycle (symbol ○). In the ordinate scale of Figure 5, the OOT is not clear.

In order to increase the sensitivity of the SAXS data near T_{OOT}, shown in Figure 5, plots of (a) $1/I_m$ vs $1/T$ and (b) σ_q^2 vs $1/T$ obtained from high-temperature-resolution SAXS experiments during the heating cycle at temperatures ranging from 170 to 185 °C are given in Figure 6. Figure 6, together with Figure 5, shows a sharp discontinuous change in both $1/I_m$ and σ_q^2 vs $1/T$ plots at around 183 °C; both $1/I_m$ and σ_q^2 increase rapidly with increasing temperature above 179 °C (the onset of OOT), reach a maximum value at around 183 °C due to the coexistence of the cylindrical and spherical microdomains, and then decrease with a further increase of temperature to 185 °C, at which the OOT is completed. The increases of $1/I_m$ and σ_q^2 at 179 °C < T < 185 °C are due to the coexistence of the two morphologies. The OOT is found to occur in the temperature interval less than 6 °C.

The following observations are worth elaborating on with reference to Figures 5 and 6. In the heating cycle, Vector 4111 experiences three different morphological states separated by the OOT and LDT; namely, it has (i) hexagonally-packed cylindrical microdomains at $T < T_{OOT}$, (ii) spherical microdomains in a cubic lattice at $T_{OOT} < T < T_{LDT}$, and (iii) liquidlike spherical microdomains at $T_{LDT} < T \leq 220$ °C. In the cooling cycle, (i) Vector 4111 has liquidlike spherical microdomains at $T_{OOT} < T \leq 220$ °C, and this is a metastable state and the long-range spatial order of the spheres gradually increases with decreasing temperature, as manifested by the decrease of σ_q^2 or the decrease of $1/I_m$ with increasing $1/T$, and (ii) at $T < T_{OOT}$ Vector 4111 has hexagonally-packed cylindrical microdomains with its long-range order increasing with $1/T$, as seen in the decrease of σ_q^2 and decrease of $1/I_m$ with increasing $1/T$. In the temperature range where the PS block chains form the hexagonally-packed cylinders and the spheres in a cubic lattice, the domain size and the lattice constant should change with temperature. However, these changes are not a main issue in the present study and, hence, will not be discussed further. It should be mentioned that the LDT and the related change in the rheological properties were previously reported by Hashimoto et al.[16] for polystyrene-*block*-polybutadiene (SB diblock) copolymer in *n*-tetradecane solution, where spherical microdomains of polystyrene remained vitrified in the temperature range investigated for their study.

Figure 7 gives plots of Bragg spacing (D) vs $1/T$ for Vector 4111 at temperatures ranging from 165 to 220 °C during the heating and cooling cycles, respectively.

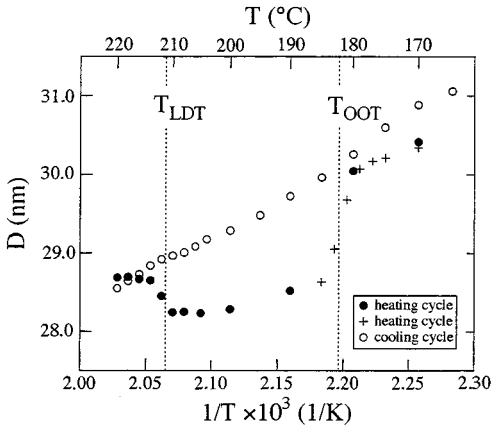

Figure 7. Plots of D vs 1/*T* for Vector 4111: (●) low-temperature-resolution SAXS experiment during heating; (+) high-temperature-resolution SAXS experiment during heating; (○) high-temperature-resolution SAXS experiments during cooling.

In Figure 7, (i) the symbol ● represents the data points taken during heating with temperature protocol 2 given in Figure 2, (ii) the symbol + represents the data taken from the high-temperature-resolution SAXS experiment during heating with temperature protocol 1 given in Figure 2, and (iii) the symbol ○ represents the data points taken from high-temperature-resolution SAXS experiments during cooling with temperature protocol 3 given in Figure 2. The following observations are worth noting in Figure 7. In the heating cycle, there are sharp changes across the T_{OOT} and T_{LDT}, respectively, and the increase of D with increasing T across the T_{LDT} is very intriguing in that this may reflect a symmetry break from cubic symmetry to the liquidlike short-range-ordered spheres. In the cooling cycle, on the other hand, no sharp changes are seen across the T_{LDT} in the time scale of our observation. However, the slope, $(\partial D/\partial T)_p$, changes across the T_{OOT} owing to a change in symmetry and also to the temperature dependence of segregation power between polystyrene (PS) and polyisoprene (PI) block chains in the two regimes at temperatures below and above the T_{OOT}.

It should be noted that OOT and LDT generally depend on the time scale of observations, as clearly revealed by the large hysteresis effects observed in the SAXS experiments conducted in the heating and cooling cycles. Thus, the time scale of observation alters the temperatures at which OOT and LDT occur, the temperature intervals between the onset and completion of the transitions, and the state of the system in between the two transitions as characterized by $1/I_m$, σ_q^2, and D.

As will be shown below in section 3.4 using theoretical prediction, the T_{ODT} of Vector 4111 is estimated to lie somewhere between 237 and 247 °C, which is not too far away from 220 °C, the highest experimental temperature employed. At 220 °C, Vector 4111 has spheres whose spatial order is destroyed, forming a liquid phase (see Figure 1d). Although during the cooling cycle the specimen was kept constant at each experimental temperature for 40−60 min, it might have required a much longer time (perhaps several hours or days) for Vector 4111 to attain an equilibrium morphology. Due to the supercooling effect (i.e., the effect of spheres being kept in disordered spatial arrangement or cylinders being kept in disordered hexagonal lattice), the liquid phase of spheres at 220 °C might have persisted until the specimen was cooled down to ca. 175 °C.

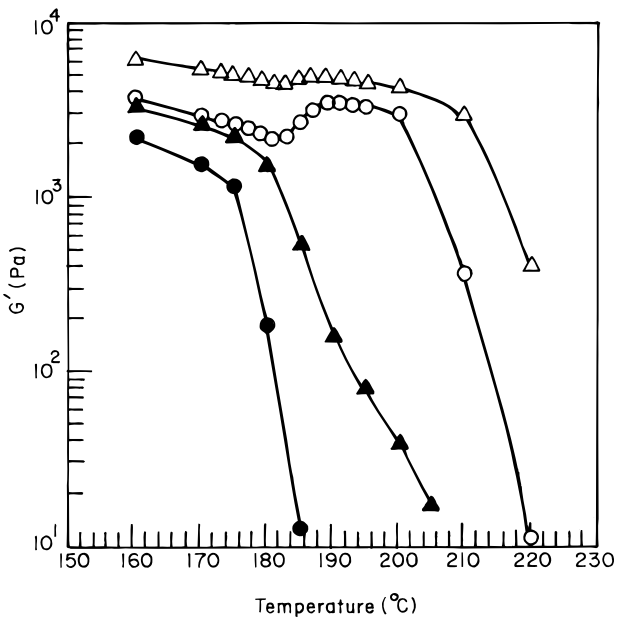

Figure 8. Temperature dependence of G' for Vector 4111 specimens, which were annealed at 140 °C for 2 days, under isochronal conditions: (a) at $\omega = 0.01$ rad/s during heating (○) and during cooling (●) and (b) at $\omega = 0.1$ rad/s during heating (△) and during cooling (▲).

3.3. Rheological Investigation. (A) Temperature Dependence of the Dynamic Storage Modulus G' under Isochronal Conditions. Figure 8 describes variations of G' with temperature for Vector 4111 specimens, which were annealed at 140 °C for 2 days, (i) at $\omega = 0.01$ rad/s during heating (○) and cooling (●) and (ii) at $\omega = 0.1$ rad/s during heating (△) and cooling (▲). Annealing at 140 °C is useful for ordering of the hexagonally-packed cylindrical microdomains as described above. The following observations are worth noting in Figure 8. (1) During heating at $\omega = 0.01$ rad/s, G' first decreases slowly with increasing temperature, going through a minimum at ca. 182 °C, then increases, going through a maximum at ca. 190 °C, and finally decreases again, first at a moderate rate with increasing temperature to ca. 206 °C and then at a much faster rate with increasing temperature further to 220 °C. In other words, during heating, there are roughly four separate regions where the temperature dependence of G' differs from each other. In this study, we chose 220 °C to be the highest experimental temperature because, according to a previous study,[15] cross-linking reactions may take place in Vector 4111 at temperatures higher than 220 °C. (2) The temperature dependence of G' at $\omega = 0.1$ rad/s during heating is very similar to that at $\omega = 0.01$ rad/s during heating, with much smaller values of a minimum and a maximum in G'. This observation indicates that the choice of angular frequency for the dynamic temperature sweep experiment under isochronal conditions plays an important role in identifying the existence of a minimum and a maximum in G' during the heating cycle. If higher values of ω had been chosen, we might have missed the existence of a minimum and a maximum in G' during the heating cycle. (3) Judging from information obtained from the SAXS results, it seems reasonable to conclude that the minimum in G' at 182 °C in the log G' vs temperature plot corresponds to the onset of OOT and the maximum in G' at 190 °C corresponds to the completion of OOT. There is a slight shift in the onset and completion temperatures (179 and 185 °C, respectively) of OOT when comparing the log G' vs temperature plots with

the SAXS results. This may be attributable to the differences in thermal history, precision in the temperature control, and time scale of observation between the two separate experiments. The minimum in G' may be interpreted as being the consequence of the following two competing effects: (i) a decrease in G' with increasing temperature may be due to the softening of hexagonally-packed PS cylinders and (ii) an increase in G' may be due to the transformation from the hexagonally-packed cylinders to the cubic-sphere phase, which in turn involves an increasing contribution of the interface to G'. G' may reach a maximum value at the completion of OOT and then decrease with a further increase of temperature due to the softening of the PS phase. (4) The temperature dependence of G' during cooling is quite different from that during heating, and there is neither a minimum nor a maximum in G' during the cooling cycle. That is, heating and cooling do not yield the same temperature dependence of G'. This difference is attributable to the hysteresis in the formation of the cubic lattice for spherical microdomains and/or the hexagonal lattice for the cylindrical microdomains; namely, the lattice distortion in the heating process is less than that in the cooling process, as discussed above.

Although not shown here due to the limitation of space, we observed that when a Vector 4111 specimen was annealed at 200 °C for 1 h and then subjected to the temperature sweep experiment under isochronal conditions at $\omega = 0.01$ rad/s during heating and cooling, the shapes of the plots of G' vs temperature were similar to those in Figure 8, the extent of a minimum and a maximum in G' not being as pronounced as that shown in Figure 8, suggesting that the annealing conditions employed for specimens also play an important role in identifying the existence of a minimum and a maximum in G'. The significance of annealing at 200 °C was pointed out above when presenting the SAXS results.

According to Bates and co-workers,[7−10] the temperature at which G' goes through a minimum in the plot of G' vs temperature during the dynamic temperature sweep experiment under isochronal conditions may be regarded as being the T_{OOT} of a block copolymer. Applying this criterion to Figure 8, we determine the T_{OOT} of Vector 4111 to be 182−185 °C. The SAXS results confirm the validity of this assessment.

In the past, a number of investigators[17−21] determined the T_{ODT} of a block copolymer by identifying the temperature at which G' drops precipitously in the plots of G' vs temperature obtained from the dynamic temperature sweep experiments under isochronal conditions. We observe from Figure 8 that use of such a criterion is hardly justifiable to determine the T_{ODT} of Vector 4111, because no sudden drop of G' at a particular temperature can be identified. When such a temperature could not be identified, some investigators[22,23] determined the T_{ODT} of a block copolymer by identifying the temperature at which a marked change in the slope of the plot of G' vs temperature occurs. When applying such a criterion[22] to Figure 8, we determine the T_{ODT} of Vector 4111 to lie somewhere between 200 and 220 °C. However, as shown above from the SAXS study, Vector 4111 at 220 °C has spherical microdomains with liquidlike spatial order. Therefore, we can conclude that Figure 8 is *not* useful to determine the T_{ODT} of Vector 4111.

(B) Frequency Dependence of the Dynamic Moduli G' and G'' at Various Temperatures. Figure 9 gives plots of log G' vs log ω and log G'' vs log ω during heating of a Vector 4111 specimen, which was annealed at 140 °C for 2 days, at temperatures ranging from 160 to 220 °C, the highest experimental temperature. In obtaining the results in Figure 9, the specimen was kept at a fixed temperature for about 45−60 min while the oscillatory shear flow experiment was conducted by varying ω from 0.01 to 100 rad/s. The following observations are worth noting in Figure 9. (1) The value of G' initially decreases with increasing temperature from 160 to 181 °C over the entire range of ω investigated. (2) However, as the temperature is increased to 185 °C, the value of G' in the terminal region becomes even greater than that at lower temperatures, 170 and 181 °C. (3) As the temperature is increased to 210 °C, the value of G' becomes less than that at 200 °C and then exhibits a large drop as the temperature is increased further to 220 °C, having a slope of slightly less than 2 in the terminal region. (4) A very unusual rheological behavior is displayed in the lower panel of Figure 9 in that (i) at temperatures from 185 to 210 °C the value of G'' in the terminal region increases with increasing temperature and (ii) as the temperature is increased further to 220 °C, the log G'' vs log ω plot shows the slope of ca. 1 in the terminal region. To the best of our knowledge, the rheological behavior shown in Figure 9 has never been reported in the literature on block copolymers. Based on the observations made

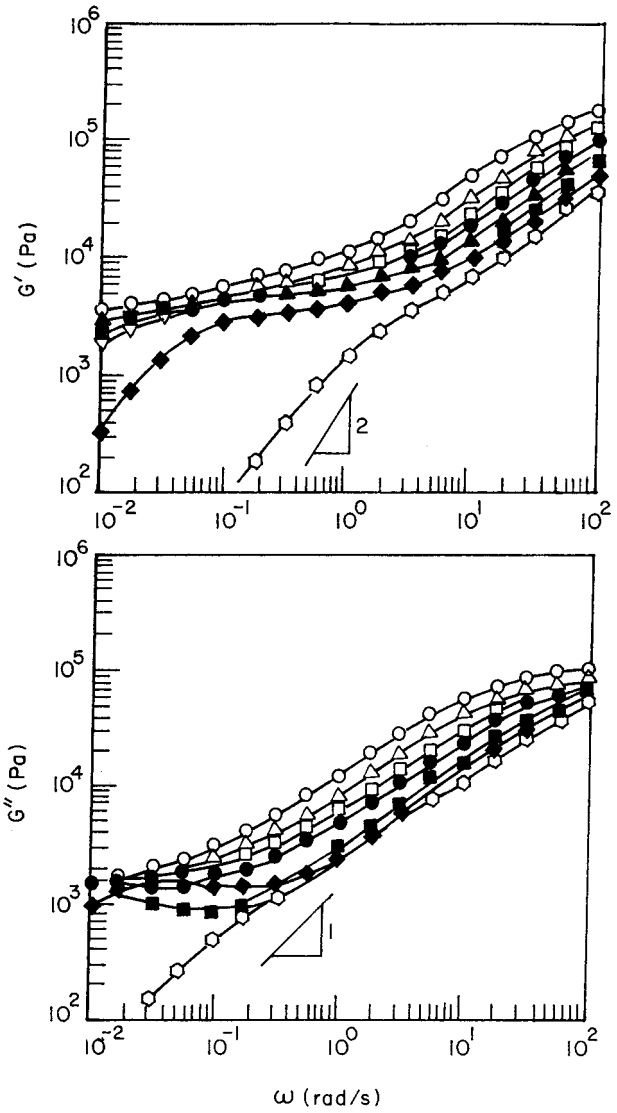

Figure 9. Plots of log G' vs log ω and log G'' vs log ω for a Vector 4111 specimen, which was annealed at 140 °C for 2 days, during *heating* at various temperatures: (○) 160 °C; (△) 170 °C; (□) 181 °C; (▽) 183 °C; (●) 185 °C; (▲) 191 °C; (■) 200 °C; (◆) 210 °C; (⬡) 220 °C.

above from Figure 9, it is very difficult to establish a rheological criterion (or criteria) for the onset of OOT or ODT.

In conjunction with the SAXS results, we can interpret these rheological behaviors as follows: observation 1 is due to the softening of the hard polystyrene cylinders with increasing temperature; observation 2 is due to OOT and increased contribution of the interface to G' and G'' in the terminal region; and observation 3 is due to an onset of LDT at 210 °C. In the temperature range where the soft-solid phase with the spheres in a cubic lattice coexists with the liquid phase with the spheres in a short-range liquidlike order, the liquidlike phase exhibits a liquidlike rheological behavior with the moduli depending on the volume fraction of the soft-solid phase, and after the completion of LDT, the moduli decrease with further increasing temperature as PS spheres soften with increasing temperature. Observations 4i and 4ii can be interpreted similarly.

It should be mentioned that in the past, some investigators[19−22] regarded a large downward shift of log G' vs log ω plots at a particular temperature as being the signature for ODT in a block copolymer. When applying such a criterion[24] to the upper panel of Figure 9, we determine the T_{ODT} of Vector 4111 to be 210 °C, and the difference in G' at 210 and 220 °C in the low-frequency region is attributed to the effect of the thermal concentration fluctuations. But, as shown above from the SAXS study, Vector 4111 at 220 °C has spherical microdomains with liquidlike spatial order. Therefore, we can conclude that Figure 9 is *not* useful to determine the T_{ODT} of Vector 4111.

Figure 10 gives plots of log G' vs log ω and log G'' vs log ω during *cooling* of a Vector 4111 specimen, which was annealed at 140 °C for 2 days, at temperatures ranging from 220 to 160°C. The following observations are noteworthy in Figure 10. (1) The slope of log G' vs log ω plots in the terminal region is ca. 2 at temperatures ranging from 220 to 185 °C but becomes very small (ca. 0.2) at temperatures ranging from 175 to 160 °C. (2) The frequency dependence of G'' in the terminal region looks somewhat similar to that of G'. Again, it is not clear from Figure 10 how to establish a rheological criterion (or criteria) for the onset of OOT or ODT.

One may be tempted to apply time−temperature superposition to obtain so-called master curves from Figure 10, as some investigators[19−23] did in the past. If such a practice were applied to the upper panel of Figure 10, we would be forced to conclude that the T_{ODT} of Vector 4111 in the cooling process is 180 °C. Such a conclusion is not tenable because our SAXS study indicates very clearly that the T_{ODT} of Vector 4111 is higher than 220 °C. The spherical microdomains clearly exist at $T > 180$ °C. It should be emphasized that Han et al.[3,25−27] already pointed out that use of time−temperature superposition to a microphase-separated block copolymer is not warranted.

A comparison of Figure 9 with Figure 10 reveals that the frequency dependence of G' and G'' during cooling is quite different from that during heating, indicating that the morphological state of Vector 4111 during cooling (i.e., the ordering process) is quite different from that during heating (i.e., the disordering process). As discussed above with reference to Figure 8, the observed differences between Figure 9 and Figure 10 are attributable to the hysteresis in the formation of the cubic lattice for the spherical microdomains and/or for the hexagonal lattice for the cylindrical microdomains; namely, the lattice distortion in the heating process is less than that in the cooling process.

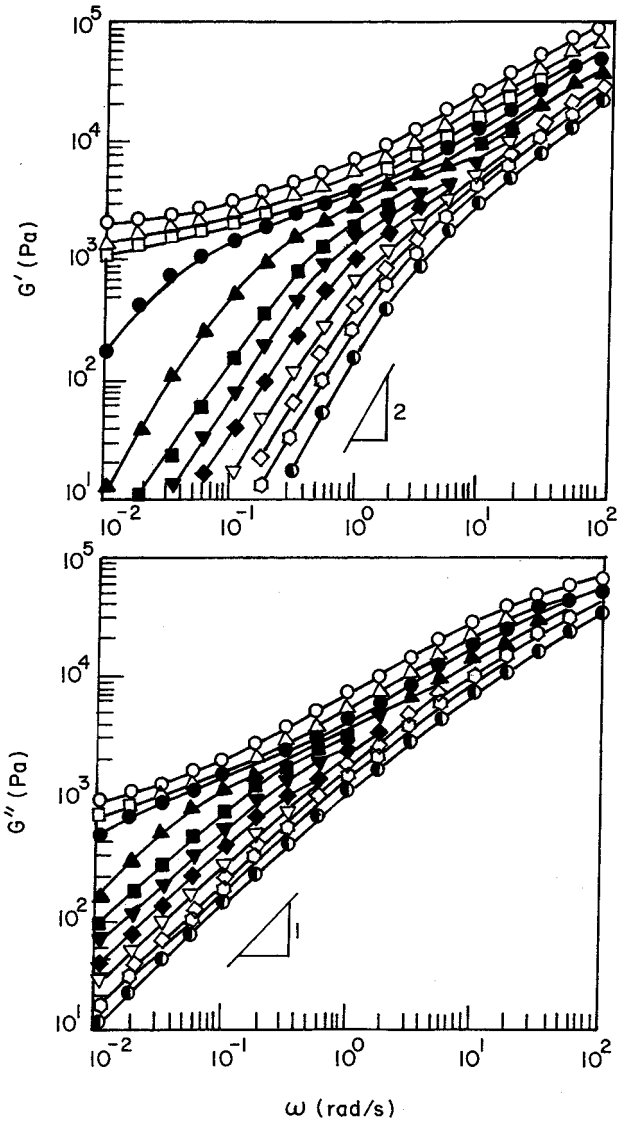

Figure 10. Plots of log G' vs log ω and log G'' vs log ω for a Vector 4111 specimen, which was annealed at 140 °C for 2 days, during *cooling* at various temperatures: (○) 160 °C; (△) 170 °C; (□) 175 °C; (●) 180 °C; (▲) 185 °C; (■) 190 °C; (▼) 195 °C; (◆) 200 °C; (▽) 205 °C; (◇) 210 °C; (⬡) 215 °C; (◐) 220 °C.

We obtained the results, similar to Figures 9 and 10, when using specimens which were annealed at 200 °C for 1 h. We thus conclude that the thermal history of the specimen, whether annealed at 140 °C for 2 days or at 200 °C for 1 h, plays little role in the frequency dependence of dynamic moduli during the cooling of Vector 4111 over the entire range of temperatures investigated, 160−220 °C. This is quite reasonable in light of the SAXS results presented above; the ordering developed upon the annealing at 140 °C for 2 days is lost when the specimen is heated to 220 °C for the rheological measurements during the cooling cycle.

(C) Plots of log G' vs log G''. Plots of log G' vs log G'' during heating for a Vector 4111 specimen, which was annealed at 140 °C for 2 days, are given in Figure 11, which was prepared using the data given in Figure 9. In Figure 11, we observe a very unusual shape for log G' vs log G'' plots. In order to facilitate our discussion here, Figure 12 is prepared by shifting the log G' vs log G'' plots given in Figure 11 along the G' axis. At temperatures ranging from 185 to 210 °C in the terminal region of Figure 12, we observe a discontinuous change in log G' vs log G'' plots having a *negative* slope, rheological behavior that has never been

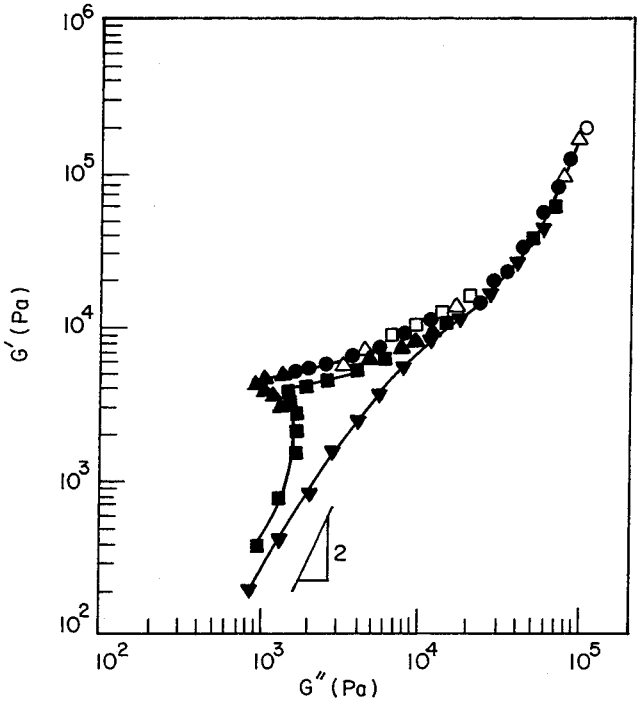

Figure 11. Plots of log G' vs log G'' for a Vector 4111 specimen, which was annealed at 140 °C for 2 days, during *heating* at various temperatures: (○) 160 °C; (△) 170 °C; (□) 183 °C; (●) 185 °C; (▲) 200 °C; (■) 210 °C; (▼) 220 °C.

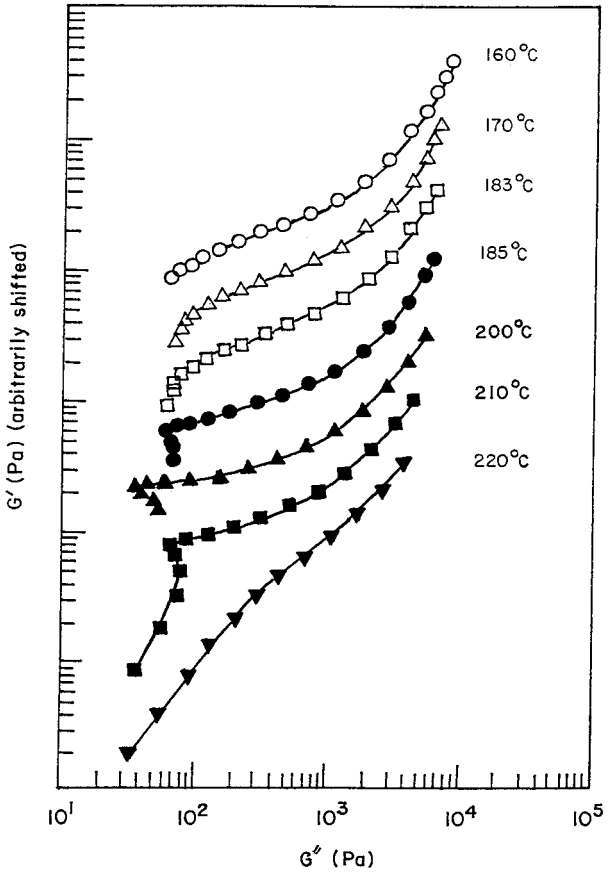

Figure 12. Plots of log G' vs log G'' for a Vector 4111 specimen, which was annealed at 140 °C for 2 days, during *heating*, in which the values of G' are shifted arbitrarily in the vertical direction in order to avoid crowdedness.

reported in the literature on block copolymers. It is of great interest to note in Figure 12 that the threshold temperature at which log G' vs log G'' plots in the terminal region begin to exhibit a negative slope is ca.

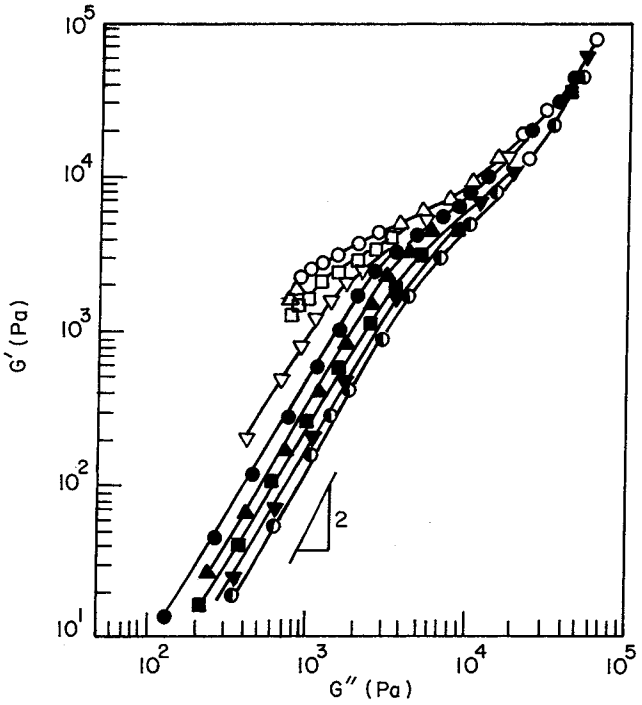

Figure 13. Plots of log G' vs log G'' for a Vector 4111 specimen, which was annealed at 140 °C for 2 days, during *cooling* at various temperatures: (○) 160 °C; (△) 170 °C; (□) 175 °C; (▽) 180 °C; (●) 185 °C; (▲) 190 °C; (■) 200 °C; (▼) 215 °C; (◐) 220 °C.

185 °C, which corresponds roughly to the temperature at which a minimum in G' was observed in Figure 8. The SAXS results suggested that this temperature corresponds to the onset of OOT. We thus conclude that log G' vs log G'' plots can be used to determine the T_{OOT} of a block copolymer. To the best of our knowledge, such a rheological criterion has never been suggested in the literature. More experiments are needed to confirm whether such a rheological criterion may be valid for other block copolymers. Judging from the SAXS results presented above, the temperature range between 185 and 210 °C with the negative slope in the log G' vs log G'' plots corresponds to that in which spherical microdomains in a cubic lattice exist, and the change in rheological behavior at 210 and 220 °C corresponds, in accordance with the SAXS results shown above, to the LDT.

Since in the terminal region of Figure 11 no two curves having a slope of 2 overlap each other, we conclude in accordance with the rheological criterion advocated by Han and co-workers[25−27] that Vector 4111 has not attained the disordered state with increasing temperature from 160 to 220 °C and, thus, the T_{ODT} of Vector 4111 is higher than 220 °C. This conclusion is in complete agreement with that drawn from the SAXS study presented above. Notice in Figure 11 that the log G' vs log G'' plot at 210 °C still has a *negative* slope in the terminal region.

The data given in Figure 10 was used to prepare plots of log G' vs log G'' for a Vector 4111 specimen during the cooling of a Vector 4111 specimen, which was annealed at 140 °C for 2 days, and are given in Figure 13. Although not shown here due to the limitation of space, we obtained very similar plots for a specimen which was annealed at 200 °C for 1 h, and thus, we conclude that the thermal history of the specimens, whether annealed at 200 °C for 1 h or at 140 °C for 2 days, affects little the temperature dependence of the log G' vs log G'' plots during the cooling of a Vector 4111

Table 2. Summary of Predicted T_{ODT} for Vector 4111

expression for the interaction parameter	eq	ref	predicted T_{ODT}, °C: Helfand–Wasserman theory	predicted T_{ODT}, °C: Mayes–Olvera de la Cruz theory[a]
$\alpha = -0.00118 + 0.839/T$	1	27	247	271
$\alpha = -0.0009 + 0.75/T$	2	32	295	327
$\chi = -0.0937 + 66/T$	3	33	212	237
$\chi = -0.0410 + 38.54/T$	4	34	185	223

[a] In the estimation of T_{ODT}, the following expression for V_r was used: $V_r = \{([M]_S v_{PS})([M]_I v_{PI})\}^{1/2}$, where $[M]_S$ and $[M]_I$ are the molecular weights of styrene and isoprene monomers, respectively, and v_{PS} and v_{PI} are the specific volumes of polystyrene (PS) and polyisoprene (PI), respectively.

specimen. In view of that fact that in Figure 13 log G' vs log G'' plots show temperature dependence at temperatures ranging from 160 to 220 °C, we conclude in accordance with the rheological criterion advocated by Han and co-workers[25–27] that the T_{ODT} of Vector 4111 is higher than 220 °C.

We observe very distinct differences between the log G' vs log G'' plots obtained during cooling (see Figure 13) and those obtained during heating (see Figure 11). It should be mentioned at this juncture that some investigators[19,20,22] have interpreted the parallel feature of log G' vs log G'' plots having a slope of 2, as the one shown in Figure 13, as being the signature for thermal fluctuation effects in the disordered state near the T_{ODT} of a block copolymer. With reference to Figure 13, there are two major problems with accepting such an interpretation. (1) We observe from Figure 13 that the T_{ODT} of Vector 4111 is higher than 220 °C, the highest experimental temperature, and thus we have no way of knowing near which temperature the thermal fluctuation effects might be significant. (2) Such an interpretation leads us to conclude that the thermal fluctuation effects for Vector 4111 near its T_{ODT} extend over 40 °C above T_{ODT}, spanning from ca. 180 °C to a temperature higher than 220 °C. On the other hand, there is ample experimental evidence in the literature,[3,23,26–29] suggesting that the thermal fluctuation effects for an SI diblock or SIS triblock copolymer near its T_{ODT} exist in the temperature interval not greater than 3–5 °C above T_{ODT}. The parallel feature of log G' vs log G'' plots observed in Figure 13 may signify that the Vector 4111 during cooling from 220 to ca. 185 °C, according to the SAXS results presented above, exhibits liquidlike rheological behavior in the terminal region due to the flow of the spherical microdomains in liquidlike spatial order. It should be emphasized that we cannot simply determine T_{ODT} from the data shown in Figure 13 and that we cannot ascribe the parallel feature of log G' vs log G'' plots from 220 to 185 °C to the thermal fluctuation effects in the disordered state.

3.4. Theoretical Prediction of the T_{ODT} of Vector 4111. Above we have shown that the T_{ODT} of Vector 4111 is higher than 220 °C. In order to corroborate the experimental results, we estimated the T_{ODT} of Vector 4111 using the currently held theories due to Helfand and Wasserman[30] and Mayes and Olvera de la Cruz.[31] As pointed out previously,[3,26,27] an estimation of T_{ODT} using these theories depends much on the particular expression used for the interaction energy density α or the Flory–Huggins interaction parameter χ, where α and χ are related to each other by $\chi = \alpha V_r$, with V_r being the molar volume of a reference component. Note that α has units of mol/cm^3 and χ is dimensionless.

Table 2 gives a summary of the estimated values of T_{ODT} of Vector 4111 using the theories referred to above, together with the expressions (eqs 1–4) used for α or χ in each theory. Also, the following expressions were used for the temperature dependence of the specific volume

$$v_{PS} = 0.9199 + 5.098 \times 10^{-4}(T - 273) + 2.354 \times 10^{-7}(T - 273)^2 + (32.46 + 0.1017(T - 273))/M_{w,PS} \quad (5)$$

for polystyrene,[35] where $M_{w,PS}$ is the molecular weight of polystyrene, and

$$v_{PI} = 1.0771 + 7.22 \times 10^{-4}(T - 273) + 2.46 \times 10^{-7}(T - 273)^2 \quad (6)$$

for polyisoprene.[26] Note in eqs 5 and 6 that v_{PS} and v_{PI} have units of cm^3/g. It can be seen in Table 2 that the estimated values of T_{ODT} vary with the expression for α or χ for a specific theory and that the estimated value for T_{ODT} (247 °C) from the Helfand–Wasserman theory together with eq 1 and the estimated values for T_{ODT} (223–237 °C) from the Mayes–Olvera de la Cruz theory together with eq 3 or eq 4 tend to support the experimental results presented above; i.e., the T_{ODT} of Vector 4111 is higher than 220 °C.

It should be mentioned that the expressions for α, eqs 1 and 2, appearing in Table 2 were obtained from the turbidity measurements for binary mixtures of oligomeric PS and PI, while the expressions for χ, eqs 3 and 4, appearing in Table 2 were obtained from the SAXS measurements for SI diblock copolymers. It has been our experience[3,26,27] that (a) the use of α values obtained from turbidity measurements in the Helfand–Wasserman theory[30] and the use of χ values obtained from SAXS measurements in the Leibler theory[11] predict a reasonable approximation of the T_{ODT} of a diblock copolymer and (2) the value of T_{ODT} predicted from the Leibler theory is higher than that from the Helfand–Wasserman theory. The readers are reminded that the Mayes–Olvera de la Cruz theory for an ABA-type triblock copolymer, which was employed in this study, is an extension of the Leibler theory for an AB-type diblock copolymer, which is based on random-phase approximation in the context of mean-field approximation. Therefore, we expect that the Mayes–Olvera de la Cruz theory would have the same degree of accuracy in its prediction of T_{ODT} as the Leibler theory.

4. Concluding Remarks

In this paper, using SAXS, we have shown that Vector 4111 (i) has hexagonally-packed cylindrical microdomains of PS at $T \leq 179$ °C, (ii) undergoes an OOT at 179–185 °C, (iii) has the coexistence of cylindrical and spherical microdomains of PS at 180 °C $\leq T \leq$ 185 °C, (iv) has spherical microdomains of PS in a cubic lattice at 185 °C $< T <$ 210 °C, (v) undergoes an LDT at temperatures between 210 (onset) and 214 °C (completion), where the cubic lattices of the spheres are distorted, and (vi) has the spherical microdomain structure of PS with a liquidlike short-range order persisting even up to 220 °C, the highest experimental temperature employed. The SAXS results are confirmed by independent TEM and rheological measurements. We believe that Vector 4111 undergoes an OOT, because the volume fraction of PS blocks ($f = 0.158$) in Vector 4111 lies near the borderline that separates the hexagonally-packed cylindrical microdomains and the spherical microdomains in the cubic lattice. It is then

reasonable to speculate that an experimental observation of OOT in a block copolymer would be very difficult when the block copolymer has a composition far away from the borderline between two microdomain structures.

We have pointed out that for the Vector 4111 investigated in this study, the distinction must be made between LDT and ODT in that (i) at temperatures above T_{LDT} but below T_{ODT}, spheres having short-range liquidlike spatial order exist and (ii) at temperatures above T_{ODT}, the spherical microdomains disappear and turn into thermal concentration fluctuations with a temperature-dependent characteristic relaxation time. It should be mentioned that the existence of LDT in a block copolymer having spherical microdomains was first reported by Hashimoto et al.[16] more than a decade ago. The sharp interface in the spherical microdomains of a block copolymer is not expected when concentration fluctuations take place in the disordered state (at $T > T_{ODT}$). At temperatures below T_{ODT}, the spheres with the sharp interface may be packed in a body-centered cubic lattice, if the random thermal force is weak compared to the force forming the lattice as in the case of the Landau-type mean-field theory.[1] In the regime where the Landau-type mean-field theory holds, LDT and ODT are identical.

We have also shown that, of the three different rheological methods presented above to investigate OOT and ODT in Vector 4111, (1) the dynamic temperature sweep experiment under isochronal conditions during heating is effective to investigate only OOT, but not ODT, whereas a similar experiment during cooling is not effective to investigate either OOT or ODT and (2) plots of log G' vs log G'' obtained during heating of a specimen are very effective to investigate both OOT and ODT. Earlier, we demonstrated that the dynamic temperature sweep experiment under isochronal conditions was very effective to investigate the ODT of SI or SIS block copolymers having ca. 50 wt % PS blocks, but not when a SI or SIS block copolymer has ca. 20 wt % or less, and 65 wt % or more, PS blocks.[3] The results of this study are consistent with the conclusions drawn from the previous studies.[3,27] Thus, the effectiveness of the dynamic temperature sweep experiment under isochronal conditions to investigate ODT in a block copolymer appears to depend very much on the block copolymer composition. On the basis of this observation, one must be wary of using the dynamic temperature sweep experiment under isochronal conditions to determine the T_{ODT} of block copolymers having low or high weight (or volume) fractions of PS blocks in a SI diblock or SIS triblock copolymer. If TEM results (Figure 1), SAXS results (Figures 3−7), or log G' vs log G'' plots (Figures 11 and 13) were not available, we might have concluded from Figure 8 that the T_{ODT} of Vector 4111 lies somewhere between 200 and 220 °C, thus forming a homogeneous state at 220 °C, which certainly is *not* true.

Since the rheological measurements cannot reveal the type of microdomain structure when Vector 4111 undergoes OOT, we conducted TEM and SAXS experiments. Our SAXS experiments reveal that Vector 4111 undergoes a morphological transition from the hexagonally-packed cylindrical to the spherical microdomains in a cubic lattice at a temperature between 179 (onset of OOT) and 185 °C (completion of OOT), and its T_{ODT} is higher than 220 °C, the highest experimental temperature employed owing to the possibility of inducing cross-linking reactions at higher temperatures. LDT was shown to give a transition in the low-frequency rheological properties from a soft solidlike behavior to a liquidlike behavior.

References and Notes

(1) Hashimoto, T. In *Thermoplastic Elastomers*; Legge, N. R., Holden, G., Schroeder, H. E., Eds.; Hanser: Munich, 1987; Chapter 12, Section 3 and references cited therein. Hashimoto, T. In Thermoplastic Elastomers, 2nd ed.; Holden, G., Legge, N. R., Quirk, R., Schroeder, H. E., Eds.; Hanser: Munich, 1996; Chapter 15A and references cited therein.
(2) Bates, F. S.; Fredrickson, G. H. *Annu. Rev. Phys. Chem.* **1990**, *41*, 525 and references cited therein.
(3) Han, C. D.; Baek, D. M.; Kim, J. K.; Ogawa, T.; Sakamoto, N.; Hashimoto, T. *Macromolecules* **1995**, *28*, 5043.
(4) Sakurai, S.; Momii, T.; Taie, K.; Shibayama, M.; Nomura, S.; Hashimoto, T. *Macromolecules* **1993**, *26*, 458.
(5) Sakurai, S.; Kawada, H.; Hashimoto, T.; Fetters, L. J. *Proc. Jpn. Acad.* **1993**, *67B*, 13; *Macromolecules* **1993**, *26*, 5796.
(6) Hajduk, D. A.; Gruner, S. M.; Rangarajan, P.; Register, R. S.; Fetters, L. J.; Honeker, C.; Albalak, R. J.; Thomas, E. L. *Macromolecules* **1994**, *27*, 490.
(7) Almdal, K.; Koppi, K. A.; Bates, F. S.; Mortensen, K. *Macromolecules* **1992**, *25*, 1743.
(8) Hamley, I. W.; Koppi, K. A.; Rosedale, J. H.; Bates, F. S.; Almadal, K.; Mortensen, K. *Macromolecules* **1993**, *26*, 5659.
(9) Förster, S.; Khandpur, A. K.; Zhao, J.; Bates, F. S.; Hamley, I. W.; Ryan, A. J.; Bras, W. *Macromolecules* **1994**, *27*, 6922.
(10) Khandpur, A. K.; Förster, S.; Bates, F. S.; Hamley, I. W.; Ryan, A. J.; Bras, W.; Almdal, K.; Mortensen, K. *Macromolecules* **1995**, *28*, 8796.
(11) Leibler, L. *Macromolecules* **1980**, *13*, 1602.
(12) (a) Hashimoto, T.; Suehiro, S.; Shibayama, M.; Saijo, K.; Kawai, H. *Polym. J.* **1981**, *13*, 501. (b) Suehiro, S.; Saijo, K.; Ohta, Y.; Hashimoto, T.; Kawai, H. *Anal. Chim. Acta* **1986**, *189*, 41.
(13) Fujimura, M.; Hashimoto, T.; Kawai, H. *Mem. Fac. Eng., Kyoto Univ.* **1981**, *43* (2), 224.
(14) Hendricks, R. W. *J. Appl. Crystallogr.* **1972**, *5*, 315.
(15) Han, J. H.; Feng, D.; Choi-Feng, C.; Han, C. D. *Polymer* **1995**, *36*, 155.
(16) Hashimoto, T.; Shibayama, M.; Kawai, H.; Watanabe, H.; Kotaka, T. *Macromolecules* **1983**, *16*, 361.
(17) Gouinlock, E. V.; Porter, R. S. *Polym. Eng. Sci.* **1977**, *17*, 534.
(18) Chung, C. I.; Lin, M. I. *J. Polym. Sci., Polym. Phys. Ed.* **1978**, *16*, 545.
(19) Bates, F. S. *Macromolecules* **1984**, *17*, 2607.
(20) Rosedale, J. H.; Bates, F. S. *Macromolecules* **1990**, *23*, 2329.
(21) Winey, K. I.; Gobran, D. S.; Xu, Z.; Fetters, L. J.; Thomas, E. L. *Macromolecules* **1994**, *27*, 2392.
(22) Adams, J. L.; Graessley, W. W.; Register, R. A. *Macromolecules* **1994**, *27*, 6026.
(23) Riise, B. L.; Fredrickson, G. H.; Larson, R. G.; Pearson, D. S. *Macromolecules* **1995**, *28*, 7653.
(24) We are of the opinion that there is no physical (or rheological) justification for using this criterion for determining the T_{ODT} of a block copolymer.
(25) Han, C. D.; Kim, J. *J. Polym. Sci., Polym. Phys. Ed.* **1987**, *25*, 1741.
(26) Han, C. D.; Kim, J.; Kim, J. K. *Macromolecules* **1989**, *22*, 383.
(27) Han, C. D.; Baek, D. M.; Kim, J. K. *Macromolecules* **1990**, *23*, 561.
(28) Gehlsen, M. D.; Bates, F. S. *Macromolecules* **1993**, *26*, 4122.
(29) Floudas, G.; Hadjichristidis, N.; Iatrou, H.; Pakula, T.; Fischer, E. W. *Macromolecules* **1994**, *27*, 7735.
(30) Helfand, E.; Wasserman, Z. R. In *Developments in Block Copolymers;* Goodman, I., Ed.; Applied Science: New York, 1982; Chapter 4.
(31) Mayes, A. M.; Olvera de la Cruz, M. *J. Chem. Phys.* **1989**, *91*, 7228.
(32) Rounds, N. A. Thermodynamics and Phase Equilibria of Polystyrene−Polydiene Binary Mixtures. Doctoral Dissertation, University of Akron, Akron, OH, 1971.
(33) Mori, K.; Hasegawa, H.; Hashimoto, T. *Polym. J.* **1985**, *17*, 799.
(34) Hashimoto, T.; Ijichi, Y.; Fetters, L. J. *J. Chem. Phys.* **1988**, *89*, 2463.
(35) Richardson, M. J.; Savill, N. G. *Polymer* **1977**, *18*, 3.

MA960610C